

The anaerobic oxidation of methane and sulfate reduction in sediments from Gulf of Mexico cold seeps

Samantha B. Joye^{a,b,*}, Antje Boetius^{c,d,e}, Beth N. Orcutt^a, Joseph P. Montoya^f,
Heide N. Schulz^{g,1}, Matthew J. Erickson^a, Samantha K. Lugo^a

^aDepartment of Marine Sciences, University of Georgia, Athens, GA, USA

^bHanse Institute for Advanced Study, 27753 Delmenhorst, Germany

^cAlfred Wegener Institute for Polar and Marine Research, 27515 Bremerhaven, Germany

^dInternational University Bremen, 28759 Bremen, Germany

^eMax Planck Institute for Marine Microbiology, 28359 Bremen, Germany

^fSchool of Biology, Georgia Institute of Technology, Atlanta, Georgia, USA

^gDepartment of Microbiology, University of California, Davis, California, USA

Received 20 December 2002; received in revised form 13 April 2003; accepted 23 December 2003

Abstract

We determined the geochemical characteristics of sediments and measured rates of the anaerobic oxidation of methane (AOM) and sulfate reduction (SR) in samples collected near thermogenic (structure II) gas hydrate mounds and in areas lacking hydrates along the continental slope in the Gulf of Mexico. We used radiotracer (C-14 and S-35) techniques to determine rates of AOM and SR over depth in sediment cores. Abundant mats of white and orange *Beggiatoa* spp. were common in areas of active seepage and these sediments were enriched in hydrogen sulfide and methane. In cores collected from areas without *Beggiatoa* or hydrate, concentrations of redox metabolites showed little variation over depth and these sites were inferred to be areas of low seepage. Integrated AOM rates were low in *Beggiatoa*-free cores ($<0.05 \text{ mmol m}^{-2} \text{ day}^{-1}$) and averaged $2.8 \pm 4.6 \text{ mmol m}^{-2} \text{ day}^{-1}$ in seep cores that contained *Beggiatoa* or gas hydrate. Integrated SR rates were also low in *Beggiatoa*-free cores ($<1 \text{ mmol m}^{-2} \text{ day}^{-1}$) and averaged $54 \pm 94 \text{ mmol m}^{-2} \text{ day}^{-1}$ in cores with *Beggiatoa* or hydrate. Rates of SR generally exceeded rates of AOM and the two processes were loosely coupled, suggesting that the majority of SR at Gulf of Mexico hydrocarbon seep sites is likely fueled by the oxidation of other organic matter, possibly other hydrocarbons and oil, rather than by AOM.

© 2004 Elsevier B.V. All rights reserved.

Keywords: Anaerobic oxidation of methane; *Beggiatoa*; Cold seeps; Nutrients; Sulfate reduction

1. Introduction

Gas hydrates are solid ice-like structures, made up of gas (predominantly methane) encaged inside ice crystals. They are stable at low temperatures ($<10 \text{ }^\circ\text{C}$) and high pressures ($\geq 5 \text{ MPa}$). Gas hydrates represent an important and dynamic organic carbon

* Corresponding author. Department of Marine Sciences, University of Georgia, Room 220 Marine Sciences Building, Athens, GA 30602-3636, USA. Tel.: +1-706-542-5893; fax: +1-706-542-5888.

E-mail address: mjoye@arches.uga.edu (S.B. Joye).

¹ Current address: Institute of Microbiology, University of Hannover, Hannover, Germany.

reservoir on the Earth and the amount of methane in gas hydrates probably exceeds reserves of conventional oil and gas (Collett and Kuuskraa, 1998). Most of the gas hydrates on the Earth occur in the oceans, and most of the hydrates in the ocean occur along continental margins (Kvenvolden, 1988). Methane seeps and associated gas hydrates occur along both active (e.g., the Cascadia margin, Suess et al., 1999; the Nankai trough Ashi et al., 2002; Tsunogai et al., 2002; the Costa Rican margin, MacDonald et al., 1996; Kahn et al., 1996; the Peru-Chile triple junction, Brown et al., 1996) and passive (e.g., the Blake Plateau, Dickens et al., 1997; the Gulf of Mexico, Kennicutt et al., 1985) continental margins.

The sediments in the northern Gulf of Mexico overlie enormous reservoirs of liquid and gaseous hydrocarbons that rest upon Jurassic-age salt deposits (Kennicutt et al., 1988a,b; Roberts et al., 1999). Salt-driven tectonics creates fault networks that serve as conduits for the rapid transfer of oil, gas and brines from deep reservoirs through the overlying sediments and ultimately into the water column (Kennicutt et al., 1988a,b; Aharon et al., 1992; Roberts and Carney, 1997). On the seafloor, such conduits give rise to gas vents and seeps, subsurface and sediment surface-breaching gas hydrates, brine pools, and mud volcanoes (Aharon, 1994; Sassen et al., 1994). Gulf of Mexico gas hydrates are structure II hydrates, containing methane (44%), ethane (11%), propane (32%), *iso*-butane (9.5%), butane (3%) and pentane (0.5%) (Sassen et al., 1998; Orcutt et al., 2004). Sediments in and around areas of active seepage are characterized by elevated concentrations of simple (C_1 – C_5) and complex (oils) hydrocarbons and hydrogen sulfide (H_2S).

Complex chemosynthetic communities comprised of a variety of microorganisms and bacteria-metazoan symbioses thrive around hydrocarbon seeps in the Gulf of Mexico (Kennicutt et al., 1985; MacDonald et al., 1989, 1990, 1996; Fisher, 1990; Ferrell and Aharon, 1994; Larkin et al., 1994). These communities proliferate in a cold, high-pressure environment by exploiting the abundance of energy-rich reduced substrates, such as methane and H_2S . While the diversity and distribution of seep macrofauna has been the focus of intense study, the activity of free-living bacteria in seep sediments and around gas hydrates has received little attention. This lack of information

is surprising given that microbial activity may impact the flux and composition of both liquid and gaseous hydrocarbons and oils as they transit the seep ecosystem (Kennicutt et al., 1988a,b; Sassen et al., 1998) and may even be responsible for the formation of seep deposits, such as carbonate reefs, chimneys, and mounds (Ferrell and Aharon, 1994; Suess et al., 1999; Michaelis et al., 2002).

Because of their occurrence along continental margins, the stability of gas hydrate reservoirs is sensitive to changes in global climate that could increase water temperatures or decrease sea level, thereby altering the hydrate stability field (Paull et al., 1991; Kvenvolden, 1993). As such, gas hydrates represent one of the most dynamic organic carbon reservoirs on Earth. Gas hydrate dissociation has been correlated with significant variations in global climate (Dickens et al., 1995; Katz et al., 1999; Norris and Röhl, 1999; Kennett et al., 2000; Hesselbo et al., 2000), suggesting that periodic pulses of hydrate-derived methane to the atmosphere contributed to past increases in global temperatures and changes in global carbon fluxes (Hesselbo et al., 2000; Kennett et al., 2000). Hence, methane oxidation in sediments near gas hydrate deposits represents a globally important biological sink for hydrate-derived methane. Understanding linkages and feedbacks between gas hydrates and global climate on a large scale requires a firm understanding of microbial methane cycling in hydrate ecosystems on a small scale.

The anaerobic oxidation of methane (AOM) and sulfate reduction (SR) are dominant microbial processes in methane-rich sediments (Hinrichs and Boetius, 2002). In marine sediments, rate measurements of SR and AOM and modeling of pore water geochemical parameters suggest that most (if not all) of the upward CH_4 flux is oxidized anaerobically near the sulfate–methane interface (Reeburgh, 1976; Devol et al., 1984; Iversen and Jørgensen, 1985). Syntrophic coupling between methane oxidizing and sulfate reducing microorganisms supposedly mediates AOM (Hoehler et al., 1994, 2001; Hoehler and Alperin, 1996). Organic geochemical biomarker and molecular biological data from marine sediments have provided further evidence that a syntrophic consortium of sulfate reducing bacteria and methanotrophic archaea mediate AOM (Hinrichs et al., 1999; Boetius et al., 2000; Orphan et al., 2001a,b; Michaelis et al.,

2002). Syntrophic metabolism as the mechanism of AOM infers that the processes of AOM and SR are closely coupled. Though multiple putative methanotrophic archaea and SO_4^{2-} -reducing bacterial (SRB) partner organisms have been identified in several environments (Hinrichs et al., 1999; Orphan et al., 2001a,b; Michaelis et al., 2002), the biochemical mechanism of the process remains unknown.

Documenting patterns of sediment biogeochemistry and microbial CH_4 processing is important because rising global temperatures could destabilize gas hydrates in shallow basins like the Gulf of Mexico where surface breaching structure II gas hydrates are abundant. Methane oxidation in the sediments and in the water column represents a sink for methane derived from hydrate dissociation and provides a mechanism to reduce the flux of hydrate-derived methane to the atmosphere (Hinrichs and Boetius, 2002). Investigating rates and controls on methane oxidation in sediments associated with gas hydrates represents a unique opportunity to elucidate how

biological oxidation influences the cycling and fate of methane in these unique habitats. Here, we present data describing the biogeochemical signature of seep sediments and the first contemporaneous measurements of the anaerobic oxidation of methane (AOM) and sulfate reduction (SR) in sediments influenced by both complex hydrocarbon and oil seepage and the presence of gas hydrates.

2. Materials and methods

2.1. Study sites

Samples were collected from sites GC185 and GC234 in the Green Canyon area of the Gulf of Mexico during a July 2001 research cruise (Fig. 1, Table 1). These sites support lush chemosynthetic communities, including free-living bacteria (*Beggiatoa*) and thiotrophic (tube worms) and methanotrophic (seep mytilids) chemosynthetic fauna. We

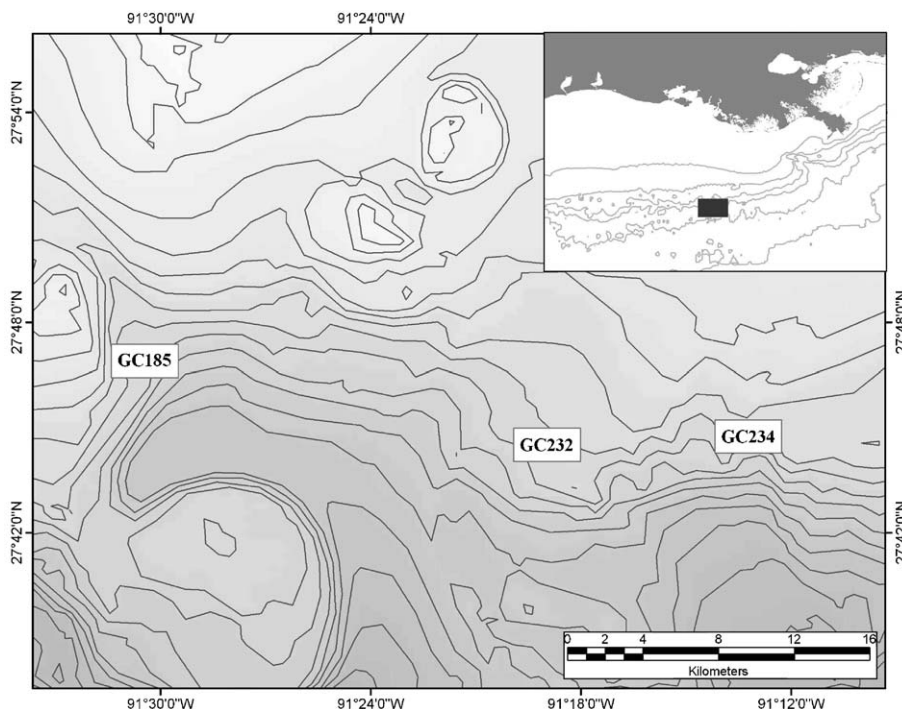


Fig. 1. Areas of active hydrocarbon and petroleum seepage are abundant along the continental slope of the Gulf of Mexico. The inset shows the coastline of Louisiana and the dark box marks the region expanded in the main map. The depth contours on the main map reflect 50-m intervals. Study sites discussed in this paper [GC185 and GC234] are marked.

Table 1

Locations of study sites and brief descriptions of cores from which data are presented

Site ID	Latitude, longitude	Depth (m)	Seepage	Core	Description
GC185	27°46.9' N, 91°30.4' W	560	oil and gas	4309	orange <i>Beggiatoa</i>
			oil and gas	4324	hydrate
			low seepage	4307	on-site control
			low seepage	4308	on-site control
GC234	27°44.1' N, 91°13.1' W	540	oil and gas	4313	white <i>Beggiatoa</i>
			oil and gas	4315	white <i>Beggiatoa</i>
			oil and gas	4316	white <i>Beggiatoa</i>

GC185 and GC234 are both gas hydrate-dominated sites.

collected samples from sediments near gas hydrates where mats of giant sulfur oxidizing bacteria, such as *Beggiatoa*, were present. The presence of microbial mats served as an indicator of high pore water H₂S concentration and inferred high rates of advection indicating *active* seepage areas. Cores collected in areas that lacked signatures of seepage, such as gas bubbles emanating from sediments, chemosynthetic communities, bacterial mats, buried and exposed hydrate mounds, and/or carbonate crusts were used as low flux (control) cores. It is important to note that these cores are not necessarily from areas lacking seepage. However, seepage in low flux areas was not high enough to support microbial mats or metazoan communities. Such samples are referred to as *low seepage cores* in this paper. Sediment push cores were collected into custom piston barrels connected to butyrate core liners that were positioned using the robotic arm of the deep submergence vessel *Johnson Sea-Link*. Typically six to nine cores ranging in length from 10 to 25 cm were collected during a dive. Upon return to the surface, cores were transferred immediately to an environmental lab held at bottom water temperature (~ 8 °C). There, cores were examined and photographed and cores with a level sediment–water interface were allocated for use in various analyses/measurements. All subsequent core processing was conducted in the environmental lab at 8 °C.

2.2. Core sectioning

For collection of samples from discrete sediment depths, the core tube was fitted with a piston (black rubber stopper) and mounted on a hydraulic extruder. The sediment was extruded at intervals (1 cm in the top 7 cm, and 3- to 5-cm layers below 7 cm) into an argon filled glove bag. As a new layer was extruded, a 2-cc sub-core was collected into a cut-off syringe and immediately transferred to a 10-ml helium-purged vial that contained 4 ml of helium-purged 2 M NaOH, which served to stop biological activity in the sample. This sample was used to quantify dissolved CH₄ concentration. Next, a 1-cc sub-sample was collected for the determination of porosity (determined by the change in weight after drying at 80 °C). The remaining sediment was transferred to a Reeburgh-type squeezer for pore water extraction (Reeburgh, 1967).

Individual squeezer sample cups were machined from solid PVC and put through several cycles of acid/base treatment followed by copious milli-Q® water rinses before use. Each cup was equipped with acid-cleaned, milli-Q® water-rinsed, dry latex rubber sheets, Teflon o-rings and ashed-glass fiber (0.8 µm optimal pore size) filters. The squeezer pressure was maintained at 20 psi (argon) and the pore water that passed through the GFF filter was collected into a gas tight glass syringe with care to avoid bubbles. A pore water sub-sample was subsequently filtered through a milli-Q® water-rinsed, air-dried 0.2-µm Acrodisc® syringe filter. All samples were stored in glass vials with Teflon-lined caps and kept refrigerated until analysis. After squeezing, the sediment was placed into a whirl-pack bag. Each bag was purged subsequently with Argon, sealed without a headspace, and then frozen.

2.3. Dissolved components

The concentration of dissolved methane was determined by vigorously shaking samples to assure transfer of gas from the dissolved phase to the headspace. A 1-cc headspace sub-sample was injected into a Shimadzu gas chromatograph. A temperature ramp was employed to separate methane from other hydrocarbons on a Hayes-Sep-D® column (2 m) and a flame ionization detector, which quantified sample signals. Certified standard gas mixtures (0.1% and

10% CH₄ in a balance of He) served to calibrate the GC signals for methane. Analytical precision was better than 1.5%. For the following analyses of dissolved components, appropriate blanks and internal standards (as noted) were run routinely and sample concentrations were determined by comparison to a standard curve generated from certified standards. A 1-ml sub-sample for the quantification of total dissolved hydrogen sulfide (H₂S) concentration was transferred to a vial containing an equal volume of 20% zinc acetate (ZnAc). Hydrogen sulfide concentration was determined using colorimetry (Cline's reagent; Cline, 1969) with a precision of 3% to 5%. Sub-samples (1 ml) for the determination of dissolved inorganic carbon (DIC) concentration were fixed and stored under a helium atmosphere prior to quantification of DIC via infrared detection on a Shimadzu TOC[®] analyzer. Precision of the analysis was 0.5% to 2%. Dissolved organic carbon (DOC) concentrations were determined on acidified (pH < 2) sub-samples using the Shimadzu TOC[®] analyzer with an analytical precision of 2% to 5%.

Samples for the determination of dissolved sulfate (SO₄²⁻) and chloride (Cl⁻) concentrations (1.5 ml) were acidified using concentrated ultrex HNO₃ (100 μl HNO₃/ml sample). Sulfate and Cl⁻ concentrations were quantified on a Dionex[®] DX5000 ion chromatograph after dilution by either 1:100 (for high SO₄²⁻ samples) or 1:10 (for low SO₄²⁻ samples). Precision of the analysis was 1.5% for SO₄²⁻ concentrations > 2 mM and 5–7% for SO₄²⁻ < 2 mM. Samples for the determination of dissolved nutrients were filter-sterilized and stored at 4 °C until analysis. Ammonium (NH₄⁺) was analyzed immediately on board ship using the indo-phenol colorimetric method (Soloranzo, 1969). The analytical precision of the analysis was usually better than 5%. Nitrate (NO₃⁻ = nitrate plus nitrite) and phosphate (PO₄³⁻) concentrations were determined using Cd-reduction followed diazotization, and the molybdate-blue methods, respectively, using an Alpkem 2-channel autoanalyzer. Precision of these analyses was about 2%.

2.4. Solid phase components

Sediment samples were dried at 60 °C and ground with a mortar and pestle before isotopic analysis. We have found that acidification frequently causes small

but variable changes in δ¹⁵N (J.P. Montoya, unpublished data), so separate samples were prepared for nitrogen and carbon isotopic analyses. For the nitrogen isotope measurement, 5 to 20 mg of ground sample was weighed into a tin capsule that was compressed using a pellet press. For the carbon isotope measurement, a sub-sample of ground sediment was acidified with 10% HCl to remove carbonates, then dried at 60 °C before being weighed into tin capsules and pelletized.

Carbon and nitrogen mass and isotopic abundance measurements were made by continuous-flow isotope ratio mass spectrometry (CF-IRMS) using a Carlo Erba NA2500 elemental analyzer interfaced to a Micromass Optima mass spectrometer. All isotope abundances are expressed as δ¹⁵N and δ¹³C values relative to accepted standards (atmospheric N₂ and V-PDB, respectively). Each analytical run included a series of elemental (acetanilide) and isotopic (peptone) standards to provide checks on instrument stability and to allow us to correct for the analytical blank in both mass and isotopic measurements. In almost all cases, the nitrogen blank was trivial relative to the samples and a blank correction was not necessary. In contrast, we found a consistent carbon blank of about 0.2 μmol C. We estimate that the overall analytical precision of isotopic measurements is ± 0.2‰ for both elements.

2.5. Microelectrode profiling and determination of bacterial biomass

Profiles of dissolved H₂S gas (H₂S_g) were obtained at in situ temperature using an H₂S_g specific microelectrode (Jeroschewski et al., 1996). Pore water profiles were determined on the same cores used to determine the biomass of vacuolate sulfur bacteria (VSB) and H₂S_g profiles. For determination of VSB biomass, a sub-core was collected into a cut-off 5-ml syringe. The sediment was subsequently pressed out of the syringe into an open petri dish in intervals corresponding to sediment depths of 0–0.25, 0.25–0.5, 0.5–1, 1–2, 2–3, 3–4 and 4–5 cm. The sediment sub-sections were suspended in seawater using a preparation needle and the total number of each type of VSB was counted under a stereo-loop. Sub-samples were taken so that the average length and diameter of VSB could be determined using a light microscope.

Total biovolume of each VSB was calculated by multiplying the average cell volume times the total cell number.

2.6. Rate measurements

For the determination of AOM and SR rates, one to six sub-cores (30-cm length \times 2.54-cm i.d.) were collected from a core. Each plexiglass sub-core had pre-drilled, silicone-sealed injection ports at 1-cm intervals along one side of the core. The water phase overlying the core was maintained during sub-coring and the ends of the core tubes were sealed with black rubber stoppers. For AOM, 10 μ l of dissolved $^{14}\text{CH}_4$ tracer (about 20,000 dpm in milli-Q water) was injected into each silicone-filled port. While time series incubations showed that AOM rates were linear for up to 48 h (Joye unpublished data), SRR rates were often nonlinear after 12–18 h (Arvidson et al., in press and Joye unpublished data). Thus, we elected to use short (12 h) incubations at bottom water temperature (8 $^\circ\text{C}$) for both AOM and SR. Following incubation, AOM sub-cores were extruded and each cm, a sub-sample was transferred to a 20-ml vial containing 5 ml of 1 M NaOH, which served to arrest biological activity and fix $^{14}\text{CO}_2$ and $\text{H}^{14}\text{CO}_3^-$. Vials were closed with a Teflon-lined screw cap, vortexed to mix the sample and base, and immediately frozen. Time zero samples were processed immediately after tracer injection and did not exhibit significant (i.e., >background) product (^{14}C -DIC) counts (data not shown). Killed controls consisted of sub-samples that were fixed with either base (for AOM) or ZnAc (for SR) prior to radiotracer addition. The product activity in killed controls was never significant. The activity of the $^{14}\text{CH}_4$ was determined by injecting 10 μ l of the tracer solution directly into scintillation cocktail. Radioactivity was determined using liquid scintillation counting (Joye et al., 1999).

The accumulation of ^{14}C product (^{14}C -DIC) was determined by acid digestion. Serum vials were opened, vented to remove $^{14}\text{CH}_4$ for 2 h and transferred to a 250-ml Erlenmeyer flask. Sample vials were rinsed twice with 5 ml of 0.1 M NaOH to remove residual sediment and fluid and the wash water was transferred to the Erlenmeyer flask. Each flask was sealed with a black rubber stopper fitted with a plastic holder that ran through the stopper and

contained a loop on the bottom. The loop suspended a 7-ml glass scintillation vial containing a glass fiber filter wick coated with 1.5 ml of phenethylamine and 0.5 ml of 0.5 M NaOH above the slurry. The slurry was acidified to pH 2 by the addition of 12 M H_2SO_4 and then shaken at 100 rpm for 120 min to trap $^{14}\text{CO}_2$ as a carbamide on the filter wick. Stripping blanks without isotope were run daily. To determine the efficiency of ^{14}C -DIC recovery during stripping, two flasks in each run were spiked with a known quantity of $\text{H}^{14}\text{CO}_3^-$ and otherwise treated as samples. The recovery efficiency averaged 95%. The rate of AOM was calculated using Eq. (1):

$$\text{AOM Rate} = \frac{[\text{CH}_4] \times \alpha_{\text{CH}_4} / t \times (\text{DPM} -^{14}\text{CO}_2)}{\text{DPM} -^{14}\text{CH}_4} \quad (1)$$

In this equation, the rate of the AOM is expressed as nmol CH_4 oxidized $\text{cm}^{-3} \text{ day}^{-1}$, $[\text{CH}_4]$ is the methane concentration (μM), α_{CH_4} is the isotope fractionation factor for AOM (1.06, Alperin et al., 1988), t is the incubation time (day), $\text{DPM} -^{14}\text{CO}_2$ is the activity of the product pool, and $\text{DPM} -^{14}\text{CH}_4$ is the activity of the substrate pool. For SR rate measurements, each port was injected with 50 μ l (about 2 μCi) of a solution comprised of $\text{Na}_2^{35}\text{SO}_4$ dissolved in milli-Q[®] water. Cores were incubated and then sectioned into 1-cm intervals as described above. Each section was transferred to a 12-ml centrifuge tube containing 5 ml of 20% ZnAc to halt microbial activity and fix H_2^{35}S as Zn^{35}S . In the laboratory, each sample was rinsed to remove $^{35}\text{SO}_4$ and then subjected to a one-step hot chromous acid digestion to recover reduced ^{35}S (Canfield et al., 1986; Fossing and Jørgensen, 1989), which was trapped as ZnS. The activity of ZnS and sulfate fractions was determined by liquid scintillation counting. The sulfate reduction rate was calculated using Eq. (2):

$$\text{SR Rate} = \frac{[\text{SO}_4] \times \alpha_{\text{SO}_4} / t \times (\text{DPM} - \text{H}_2^{35}\text{S})}{\text{DPM} -^{35}\text{SO}_4} \quad (2)$$

Here, the SR rate is expressed as $\mu\text{mol SO}_4$ reduced $\text{cm}^{-3} \text{ day}^{-1}$, α_{SO_4} is the isotope fractionation factor for sulfate reduction (1.06; Jørgensen, 1978), $[\text{SO}_4]$ is the sulfate concentration (mM), t is incubation time (day), and $\text{DPM} - \text{H}_2^{35}\text{S}$ is the activity of the

product pool, and $\text{DPM-}^{35}\text{SO}_4$ is the activity of the substrate pool added at the beginning of the experiment. Aerial rates ($\text{mmol m}^{-2} \text{day}^{-1}$) were obtained by integrating the rate profile over depth, taking into account the porosity.

3. Results

3.1. Core descriptions

Data describing advection (seepage) rates and heterogeneity in seepage rates for Gulf of Mexico cold seeps is not currently available so we used geochemical and biological indicators to identify sites with active seepage. The basic assumption is that sites with steady seepage receive ample reductant (e.g., constant fluxes of oil, hydrocarbons and/or CH_4) supplies necessary to sustain high rates of sediment metabolism that generates the H_2S required to support chemoautotrophic communities, including *Beggiatoa* and macrofauna (e.g., tube worms). Surface breaching

gas hydrates were always associated with *Beggiatoa* mats, even if macrofauna were absent. Thus, we used the presence of *Beggiatoa* and/or hydrate mounds to indicate areas having active and persistent seepage. To obtain cores from low seepage areas, we targeted places where the sediment surface was brown and oxidized and where active flow features, including *Beggiatoa* mats, chemosynthetic macrofauna, surface breaching gas hydrates, buried hydrate mounds which are visible as humps beneath the surface, and actively venting gas streams, were all absent. Areas meeting these requirements were designated low seepage sites. It is worth noting that even cores from low seepage sites could experience periodic seepage because advection is inherently variable at cold seeps.

Here, we focus on biogeochemical and rate data from three cores. Core 4315 contained a *Beggiatoa* mat and was collected near a gas hydrate mound. The sediments in the core were black, reduced and slightly oil-stained. Core 4324 was collected at the edge of a gas hydrate mound; the sediments in this core were extremely oily and gas hydrate was observed in the

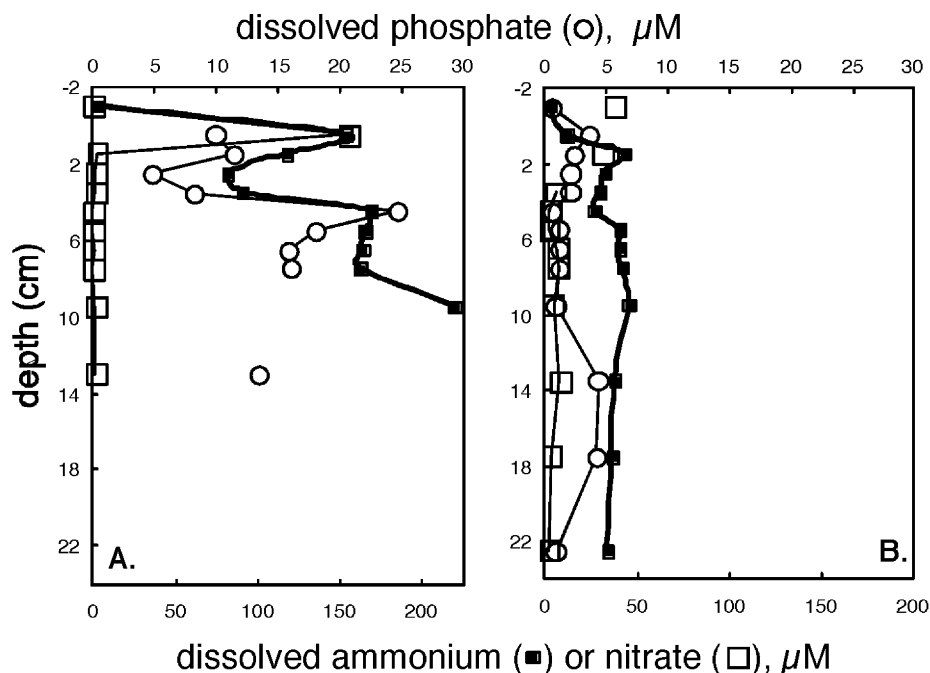


Fig. 2. Depth profiles of pore water ammonium (■), nitrate (□), and phosphate (○) concentrations from sediments near gas hydrate mounds (A: 4315) and from low seepage control site (B: 4308). Dissolved phosphate is shown on the upper axis and ammonium and nitrate are shown on the lower axis.

bottom of the core upon examination. As a result of depressurization during the return to the surface, some sublimation of the gas hydrate occurred and this led to some mixing of the pore waters. Because this core was oily and contained hydrate, it was of biogeochemical interest even though it had been disturbed during sample recovery. Thus, we allowed the core to recover for ~ 15 h in the cold room prior to sampling. Core 4308 was a low seepage control core that lacked *Beggiatoa*, contained brown, more oxidized sediment, and was not oil stained. The other cores (4307, 4309, 4313 and 4316) mentioned in this paper are described in Table 1.

3.2. Pore water nutrient concentrations and ratios

The abundance of vacuolate, nitrate-concentrating sulfur bacteria (hereafter, VSB) influenced nutrient and DOC distributions in sediment pore waters. Since it was impossible to remove VSBs from sediment prior to collecting pore water samples, the high pore water NO_3^- (and DOC) concentrations observed at depths

where VSB were abundant possibly resulted from the rupture of VSB cells during squeezing. However, the data nonetheless reflect the amount of NO_3^- and DOC in the sediment at a given depth interval, even if the material was associated with *Beggiatoa*, and clearly show that the distribution and metabolic activity of *Beggiatoa*, and probably other VSB as well, influence nitrogen, carbon and sulfur cycling in seep sediments. In general, pore water dissolved inorganic nitrogen, DIN ($\text{DIN} = \text{NO}_3^- + \text{NH}_4^+$), and dissolved inorganic phosphorus, DIP ($\text{DIP} = \text{PO}_4^{3-}$), concentrations were lower than expected from stoichiometry based on observed pore water DIC concentrations (frequently >10 mM). Pore water DIP concentrations ranged between 2 and 10 μM and DIN concentrations were 10–40 μM , except at depths where VSB were abundant (upper 1–5 cm) where DIN concentrations were up to 150 μM (Fig. 2).

DIP concentrations were similar in cores from sites with active seepage and in low activity control cores. Dissolved NH_4^+ concentrations were generally low and similar over depth in active and inactive cores (Fig. 2).

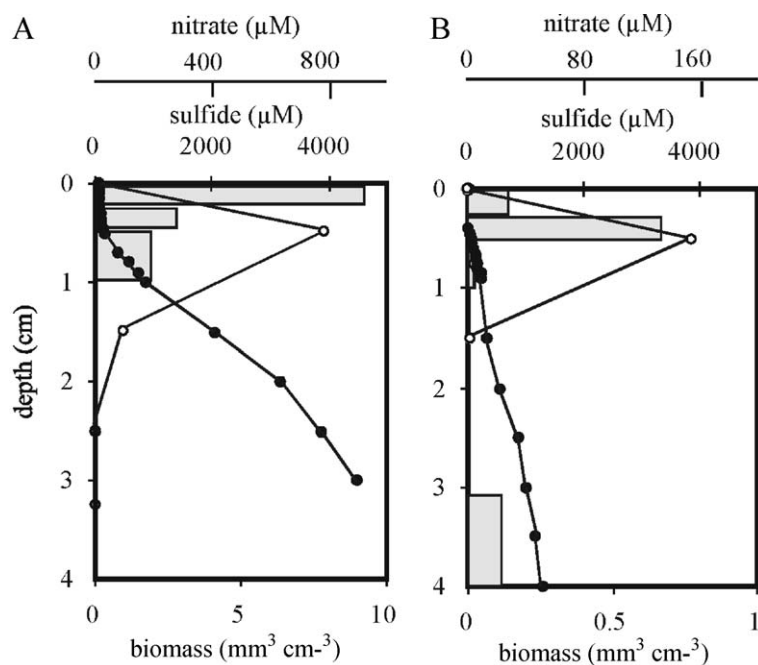


Fig. 3. Profiles of vacuolate sulfur bacteria (VSB) biomass (bars; $\text{mm}^3 \text{cm}^{-3}$; lower y-axis) and pore water concentration of hydrogen sulfide gas (sulfide, closed circles, micromolar; lower top axis) and nitrate plus nitrite (nitrate, open circles, micromolar; upper top axis). Note that the scale for NO_3^- concentration decreases from panel A (core 4314, orange *Beggiatoa*, 37–43 μm , 40 g^{-2}) to B (core 4315, white *Beggiatoa*, 31–44 μm , 5 g^{-2}). The scale for VSB biomass is an order of magnitude greater on panel A than panel B.

A surface maximum in NO_3^- concentration (and in NH_4^+ concentration in some *Beggiatoa* cores) was observed in all cores, but surface concentrations in low seepage control cores were lower than those observed in cores with VSB. The DIN/DIP ratio in low activity control cores was >50 in surface sediments (0–2 cm) and varied between 30 and 60 deeper in the core, suggesting relative P limitation. In cores with VSB, surface (1–2 cm) pore water DIN/DIP molar ratios were approximately 9–20. At depth, the DIN/DIP ratio decreased to 7–11 (N deficit relative to P). Pore water DIC/DIN (between 25 and 100) and DIC/DIP (between 500 and 1000) ratios exceeded those predicted from the oxidation of Redfield organic matter (i.e., C(106):N(16):P(1)).

3.3. Vacuolate sulfur bacteria

Abundant mats of white and orange *Beggiatoa* spp. were common at seep sites, where sediments were enriched in H_2S and CH_4 . Noticeable H_2S gradients were present in sediments with VSB and the curvature of the H_2S profiles inferred high rates of H_2S oxidation

(Fig. 3). The diameter of *Beggiatoa* filaments varied between 12 and 50 μm and the biomass varied between 3 and 74 g^{-2} . Elevated abundance of *Beggiatoa* corresponded to high concentrations of H_2S_g (Fig. 3), total H_2S (Fig. 4), and NO_3^- and DOC (Fig. 3).

3.4. Pore water redox metabolites

In low seepage control cores, concentrations of redox metabolites showed little variation over depth (Figs. 4B and 5C). Hydrogen sulfide and CH_4 concentrations in low activity cores were orders of magnitude lower (μM) than those observed in samples from sites of active seepage (mM; Fig. 5A and B) and profiles of DIC, DOC, SO_4^{2-} and H_2S were largely invariable over depth (Figs. 4B and 5C). In contrast, concentrations of DIC and H_2S were substantially elevated in sediment cores from active seeps and steep concentration gradients were observed over depth (Figs. 4A and 5A,B). Total H_2S concentrations increased rapidly with depth from tens to hundreds of micromolar in the water overlying the cores to 4 to 12 mM at depth (Fig. 5A). Similarly, DIC concentrations

dissolved inorganic (♦) and dissolved organic (○) carbon (mM)

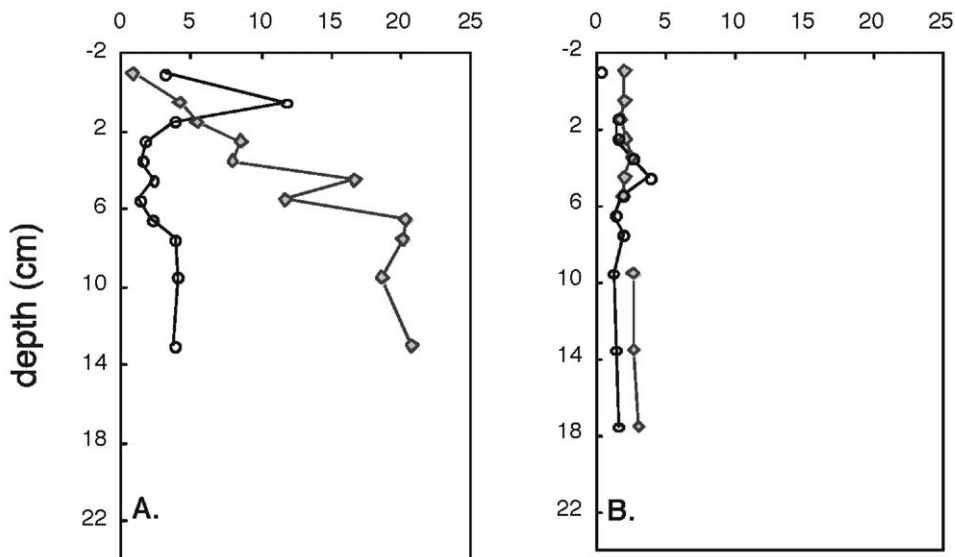


Fig. 4. Depth profiles of pore water dissolved organic carbon, DOC (○), and dissolved inorganic carbon, DIC (♦), concentrations from sediments near gas hydrate mounds (A: 4315) and from a low seepage control site (B: 4308). DIC and DOC are shown on same scale (concentration in mM).

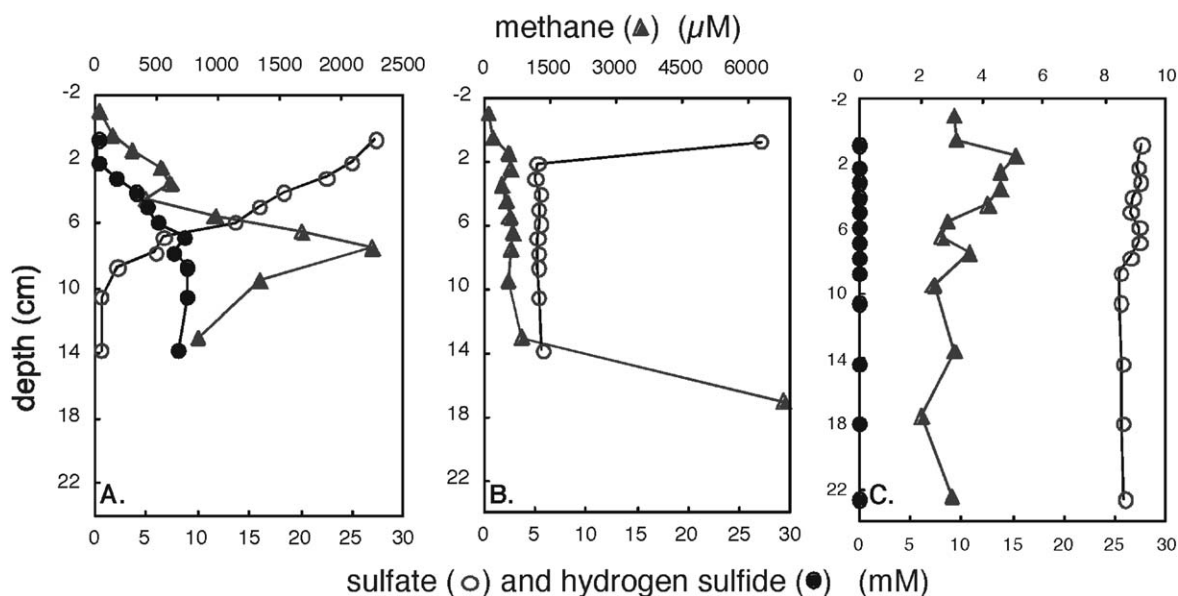


Fig. 5. Depth profiles of pore water sulfate (O), hydrogen sulfide (●) and dissolved methane (▲) concentration from sediments near gas hydrate mounds (A: 4315 and B: 4324), and from a low seepage control site (C: 4308). Note that the scale for CH_4 concentration is higher on panel B and lower on panel C. In the control core, H_2S concentration was about 20 μM all through the core.

increased from about 2 mM in the overlying water to 20 mM at depth (Fig. 4A). Pore water DOC concentrations were between 2 and 5 mM, except at depths where VSB were abundant (DOC up to 12 mM; Fig. 4A). The curvature of concentration gradients for both CH_4 and SO_4^{2-} suggests rapid rates of microbial consumption (Fig. 5A and B). In core 4315, CH_4 concentrations increased as SO_4^{2-} was depleted while in core 4324, SO_4^{2-} concentrations were rapidly depleted and remained low throughout the sediment column. Methane concentrations increased at the bottom of cores from active seep areas (Fig. 5B).

3.5. Solid phase C and N

Active seep cores were organic rich (5–10% total organic carbon, TOC; Table 2) and the C/N ratio of sediment organic matter differed significantly between cores. In core 4315, the C/N ratio increased from approximately 10 in surface sediments to approximately 20 at depth (Table 2). In core 4324, the C/N ratio increased from 20 at the surface to almost 40 at depth. The low seepage core (4308) contained <2% TOC and the C/N ratio increased from 10 (surface) to 20 (20 cm) at depth (Table 2). The fraction of

sedimentary carbon present as carbonate relative to organic carbon was similar at hydrate (40–50% in 4315 and 20% in 4324) and low seepage (20–30% in 4308) sites. Variability in the distribution of stable C and N isotopes was observed between sites. At active seep sites, the $\delta^{15}\text{N}\text{-org}$ was about 0‰. At the inactive site, the $\delta^{15}\text{N}\text{-org}$ was higher, around 2‰

Table 2

Average solid phase properties of sediments above and below 8-cm depth at active seeps (4315 and 4324) and at low seepage control (4308) sites

Core	TOC ^a	C/N ^b	$\delta^{13}\text{C}\text{-TOC}^c$	$\delta^{13}\text{C}\text{-carb}^d$	$\delta^{15}\text{N}\text{-org}^e$
4315					
0–2 cm	4	10	–23	–15	~0
> 10 cm	5	20	–25	–20	+1.2
4324					
0–2 cm	5	20	–25	–25	–0.5
> 10 cm	5–6	40	–26	–25	–1
4308					
0–2 cm	2	10	–25	–10	+2
> 10 cm	3	20	–25	–10	+2

^a Total organic carbon (weight percent).

^b Molar C/N ratio of sediment organic matter.

^c $\delta^{13}\text{C}$ of organic carbon.

^d $\delta^{13}\text{C}$ of inorganic (carbonate) carbon.

^e $\delta^{15}\text{N}$ of sediment organic matter.

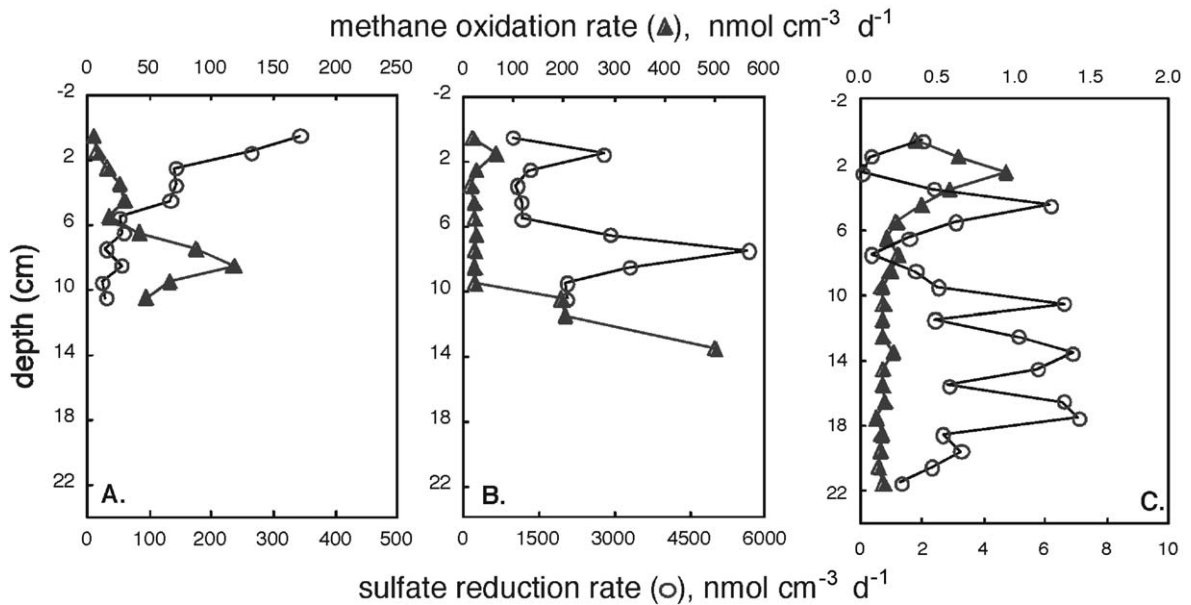


Fig. 6. Depth distribution of rates of the anaerobic oxidation of methane (\blacktriangle) and sulfate reduction (\circ) from sediments near gas hydrate mounds (A: 4315 and B: 4324) and from a low seepage control site (C: 4308). Note that the scales of the y-axes vary between panels and that the range of the AOM and SR scales are not the same.

(Table 2). The carbon isotopic composition of carbonate ($\delta^{13}\text{C}\text{-carb}$) was typically heavier than organic carbon ($\delta^{13}\text{C}\text{-org}$), except in core 4324, where both the $\delta^{13}\text{C}\text{-carb}$ and the $\delta^{13}\text{C}\text{-org}$ were approximately -25‰ at all depths. In core 4315, the $\delta^{13}\text{C}\text{-carb}$ decreased by approximately 5‰ between 0.5 and 15 cm and the $\delta^{13}\text{C}\text{-org}$ varied between -25‰ and -23‰ (Table 2). In the low seepage core, the $\delta^{13}\text{C}\text{-org}$ was about -25‰ and the $\delta^{13}\text{C}\text{-carb}$ was about -10‰ .

3.6. Rates of AOM and SR

Rates of the anaerobic oxidation of methane and sulfate reduction exhibited substantial heterogeneity (Fig. 6, Tables 3 and 4). The depth distribution of AOM and SR mirrored substrate concentrations (Figs. 5 and 6) and rates at active seeps were much higher (by 10 to 100 times) than the rates at low seepage control sites (Fig. 6). Highest rates of AOM and SR were observed in cores with the highest CH_4 concentrations

Table 3

Integrated rates of the anaerobic oxidation of methane and of sulfate reduction and estimated turnover times of the CH_4 and SO_4 pools

Core (cm)	Process	Rate within depth interval ^a				Turnover time ^b	
		total	0–5 cm	5–10	10+ cm	CH_4	SO_4
4315 (10.5 cm)	AOM	4.61	0.84	3.77	n.a. ^c	17–22	77–100
	SR	12.62	10.2	2.43	n.a.		
4324 (13.5 cm)	AOM	11.6	1.5	1.1	9.0	18–26	2–9
	SR	244.3	72.9	150.7	20.7		
4308 (22 cm)	AOM	0.056	0.029	0.009	0.017	8–19	>1000
	SR	0.727	0.108	0.091	0.526		

^a Integrated rate in $\text{mmol m}^{-2} \text{day}^{-1}$.

^b Pool turnover time [= pool (nmol cm^{-3})/rate ($\text{nmol cm}^{-3} \text{day}^{-1}$)] in days.

^c n.a. = not applicable.

Table 4

Integrated rates of the anaerobic oxidation of methane and of sulfate reduction in other cores where rates of both processes are available

Core (site)	Process	Total rate ^a	min ^b	max ^b
4307 (GC185)	AOM	0.16 to 0.28	0.3	1.3
<i>ctr</i> ^c	SR	0.01 to 0.9	0	27
4309 (GC185)	AOM	0.14 to 0.38	0.2	11.7
<i>o Begg</i> ^c	SR	18.96	98	359
4313(GC234)	AOM	0.1 to 0.38	0.2	9.7
<i>w Begg</i> ^c	SR	6.9 to 13.4	17	604
4316 (GC234)	AOM	0.34	0.3	3.4
<i>w Begg</i> ^c	SR	49.13	7	2949

^a Integrated rate in mmol m⁻² day⁻¹ (range of values shown for $n \geq 2$).

^b Minimum (min) or maximum (max) volumetric rate (nmol cm⁻³ day⁻¹).

^c *ctr*=low seepage control (no mat), *o Begg*=orange *Beggiatoa*; *w Begg*=white *Beggiatoa*.

and the most rapid SO₄²⁻ depletion over depth (Figs. 5 and 6). Surprisingly, rates of AOM rarely balanced rates of SR. Instead, integrated SR rates were typically 5–10 times higher than the integrated AOM rates (Tables 3 and 4; Fig. 6 note different scales for AOM and SR). Within distinct depth zones, however, AOM and SR rates were sometimes more closely coupled (Table 3, core 4315, 5–10 cm depth interval and core 4324, 10+ cm depth interval). Within other depth zones, coupling between the two processes was not apparent, that is, we observed high SR without concomitant elevations in AOM rates. The estimated turnover times for the CH₄ pool averaged tens of days while the estimated turnover times of the SO₄²⁻ pool varied between tens to >1000 days (Table 3). Rates of AOM and SR varied by three to five times in duplicate sub-cores from the same core. Similar variability was observed in AOM and SR rates from sub-cores representing the same type of flux regime but collected on different dives (e.g., orange *Beggiatoa*) and between cores collected from the same flux regime on different sites (again, e.g., orange *Beggiatoa*; Table 4).

4. Discussion

4.1. Biogeochemical signatures of Gulf of Mexico cold seeps

Seepage of gas and petroleum charged fluids through Gulf of Mexico sediments supports elevated

rates of microbial metabolism, resulting in distinct pore water and solid phase geochemical signatures. Microbial mats, a dynamic and vital component of seep environments in the Gulf of Mexico and elsewhere, are a good indicator of high fluid flux (Barry et al., 1996; Judd et al., 2002; Torres et al., 2002; Tyron et al., 2002). Our results show: (1) Active seep sediment metabolism is elevated significantly relative to sediments from low seepage control sites. However, oxidation of methane and other hydrocarbons and oil does not regenerate dissolved inorganic nutrients, as would be expected for other highly active organic-rich sediments. The distribution and activity of vacuolate sulfur bacteria at seep sites impact nitrogen, sulfur, and carbon, cycling significantly. (2) Rates of the anaerobic oxidation of methane and sulfate reduction were high and variable near active seeps. The turnover time for the CH₄ pool was consistently <1 month while the turnover time for the SO₄²⁻ pool varied between weeks to months at seep sites to years at low seepage sites. The high SR rates observed at seeps underscores the need for both high seepage rates and biological (oxidation of H₂S) activity to maintain substrate pools at levels capable of supporting the measured SR rates at active seeps. (3) Loose coupling between the anaerobic oxidation of methane and sulfate reduction suggests that other seep-related organic substrates, probably other hydrocarbons and oil, fuel a significant portion of sulfate reduction in these habitats.

4.2. Sediment metabolism, nutrients and vacuolate sulfur bacteria

At cold seeps, high reduced carbon fluxes fuel sulfate reduction, generating hydrogen sulfide, which serves as reductant for free-living (e.g., *Beggiatoa*, *Thiothrix*, and *Thioploca*) and symbiotic (vestimentiferan tube worms, *Escarpia* sp. and *Lamellibranchia* sp., and Lucinid clams) thiotrophs (Barry et al., 1996; Fisher, 1990). Methane fluxing from deep reservoirs into the cold seep ecosystem is consumed by aerobic free-living (de Angelis et al., 1991) and symbiotic (seep mytilids; Childress et al., 1986; Fisher, 1990) methanotrophs but a large portion of seep-derived methane is consumed by anaerobic methanotrophs within the anoxic sediments. High rates of chemosynthetic production in seep ecosystems lead to a signif-

icant transfer of carbon to higher trophic level consumers as well as to mobile predators (Carney, 1994; MacAvoy et al., 2002).

Little information on the nutrient biogeochemistry of cold seeps is available in the literature. The observed concentrations of dissolved inorganic nitrogen (DIN) and dissolved inorganic phosphorus (DIP) in active seep sediment pore waters (Fig. 2) and the elevated DIC/DIN (>25) and DIC/DIP (>300) ratios show that the majority of organic carbon oxidized in these sediments is non-Redfield (C/N/P≠ 106:16:1), nitrogen- and phosphorus-poor material, most likely, methane, hydrocarbons and oil. Gulf of Mexico seep sediments contain large amounts of hexane extractable hydrocarbons (up to 12%, Brooks et al., 1984, Kennicutt et al., 1988a). Many of the cores we collected were oil-stained and high in total organic carbon (TOC) content, ranging between 5 and 10 wt.% TOC (Table 3). Seep sediment TOC content is substantially higher than the TOC content observed at other non-seep sites in the northern Gulf of Mexico (about 1% TOC, Goñi et al., 1998). The stable isotopic signature of seep sediment TOC is about -25‰ (Fig. 6), a value lighter than typical marine organic matter (-20‰ ; Claypool and Kaplan, 1974) but is similar to the bulk isotopic signature of oils (-26‰ to -28‰) in deep Gulf of Mexico reservoirs (Kennicutt et al., 1988a).

Though some portion of the sediment organic matter could be derived from non-seep sources, either via sedimentation of autochthonous water column primary production or allochthonous terrestrial materials (see below, Goñi et al., 1998), the high TOC content, the $\delta^{13}\text{C}$ of sediment TOC, and the high DIC/DIN and DIC/DIP ratios in sediment pore waters suggest that seeping hydrocarbons and oil are the primary source of organic matter fueling SR at Gulf of Mexico cold seeps. Our study sites lie along the continental slope, where surface waters are extremely oligotrophic. We did not determine rates of water column primary production; however, given the low nutrient (Montoya, unpublished data) and low chlorophyll (0.05 to $0.5\ \mu\text{g chl } a\ \text{l}^{-1}$; Davis et al., 2002) concentrations in the water column in this area, rates of photosynthetic primary production are probably low, and thus sedimentation from this source would be negligible. Estimates of sedimentation rate in the Green Canyon region range between 1 and 60 cm/

1000 years (Behrens, 1980, 1988; Anderson et al., 1983; Hackworth and Aharon, 2002) and the average for the specific areas where we worked is reported to be about 6 cm/1000 years (Aharon and Fu, 2000). High rates of sediment metabolism, as indicated by elevated sulfate reduction rates, demonstrate an abundance of labile organic matter in seep regions. Given the low sedimentation rates documented (Aharon, 1991), it is unlikely that pelagic sedimentation could support the measured sulfate reduction rates. Even if 10-fold high estimates of sedimentation ($0.6\ \text{mm}\ \text{year}^{-1}$) occurred and if all of the sedimented material was labile organic carbon (which is unlikely), the SR rates measured at active seeps could not be maintained. Thus, most of the organic matter oxidized in the seep sediments was likely derived from the advecting organic-rich fluids.

Because of the nutrient-poor nature of the organic matter oxidized at these cold seeps, high rates of sediment metabolism do not generate large inventories of remineralized inorganic nutrients in sediment pore waters (Fig. 2). The DIN/DIP ratios of active seep sediment pore waters are suggestive of relative phosphorus limitation (Fig. 2). This suggests that DIP availability could limit accumulation of microbial biomass in cold seeps and might thereby influence the ability of seep microbial communities to efficiently consume methane and other hydrocarbons, particularly at times of high methane flux (e.g. when advection rates are high). Documenting and understanding nutrient limitation dynamics of seep microbial production requires further study.

Typical DIN profiles illustrate surface peaks in concentration of DIN, and decreasing concentrations with depth and only small (2 – $10\ \mu\text{M}$) increases with DIP over depth (Figs. 2 and 3). Potential DIN sources to benthic communities include regeneration within sediments (which does not appear to be important here), nitrogen fixation, and uptake from the water column, a process that could be stimulated by VSB activity. No data are available on nitrogen fixation rates from cold seep habitats, but Brooks et al. (1987) invoked nitrogen fixation as a possible explanation for the extremely light $\delta^{15}\text{N}$ (as low as -12‰) values observed in tissues of seep organisms. The average $\delta^{15}\text{N}$ of seep sediment organic matter (0‰ , Table 2) was lighter than the $\delta^{15}\text{N}$ of sediment organic matter ($>2\text{‰}$, Table 2) from low seepage sites, suggesting

the possibility of inputs of N via nitrogen fixation at active seeps.

Elevated bottom water concentrations of nutrients (DIN, DIP, see above, Montoya, unpublished data) could serve as a nutrient source for seep sediment microorganisms, such as *Beggiatoa*, and for macrofauna, such as tube worms or mussels. *Beggiatoa* in particular could serve as an effective nitrogen shuttle between the overlying water to the sediments. Vacuolate sulfur bacteria, like *Beggiatoa* and *Thioploca*, are abundant at cold seeps (Jannasch et al., 1989; Gundersen et al., 1992; Ahmad et al., 1999; Boetius et al., 2000). These large bacteria concentrate NO_3^- in a central vacuole and vacuole NO_3^- concentrations can be as high as 500 mM (Fossing et al., 1995; McHatton et al., 1996; Jørgensen and Gallardo, 1999). The VSB are chemoautotrophic (Nelson and Jannasch, 1983) and couple H_2S oxidation to the reduction of oxygen (*Beggiatoa*, Jørgensen and Revsbech, 1983, Nelson et al., 1986) or NO_3^- (*Thioploca*, Otte et al., 1999, and *Beggiatoa*, Sweerts et al., 1990). Whether the sulfide oxidizers of the Gulf of Mexico seeps reduce NO_3^- to NH_4^+ (Otte et al., 1999) or N_2 (Sweerts et al., 1990) remains to be determined; however, the fate of vacuole NO_3^- has important consequences for seep nitrogen budgets.

4.3. Rates of the anaerobic oxidation of methane and sulfate reduction

Areas of active seepage within Gulf of Mexico cold seeps are characterized by reduced, gas charged sediments that exhibit high rates of AOM and SR (Figs. 5 and 6). The integrated SR rates reported here were low at low seepage control sites (<1) and averaged 54 ± 94 ($n=7$, range: 3 to 244) $\text{mmol m}^{-2} \text{day}^{-1}$ in the vicinity of active seeps (Table 3 and 4). The SR rates reported here from active sites are similar to previously reported rates at Gulf of Mexico cold seeps (41 $\text{mmol m}^{-2} \text{day}^{-1}$ reported in Aharon and Fu, 2000 and 10 to 800 $\text{mmol m}^{-2} \text{day}^{-1}$ reported in Arvidson et al., in press). Our SR rates are similar also to those documented at other methane seeps (Bussman et al., 1999; Boetius et al., 2000).

The AOM rates reported here are the first directly determined (e.g., using $^{14}\text{CH}_4$ tracer) AOM rates from an active hydrocarbon seep where oil and gas hydrates are present. Integrated AOM rates were small at low

seepage control sites ($<0.05 \text{ mmol m}^{-2} \text{day}^{-1}$) and averaged 2.8 ± 4.6 ($n=8$, range: 0.1 to 12) $\text{mmol m}^{-2} \text{day}^{-1}$ at active seep sites (Table 3 and 4). Rates of AOM and the rate constants for AOM were higher at active seeps but the turnover times for the methane pool were similar at active and low seepage sites (Figs. 5 and 6). These data suggest that anaerobic methanotrophs are present even at sites experiencing ephemeral seepage and further infer that AOM rates are probably CH_4 -limited. At seep sites, pore water CH_4 concentration is correlated to the fluid flow rate (Torres et al., 2002), so AOM rates would be predicted to be maximal in areas with the highest advection rates. Fluid flow also impacts the presence of hydrates, and hydrate dissociation can also provide substrate (CH_4) for AOM, so the relative importance of fluid flow in controlling AOM rates becomes even more obvious. Torres et al. (2002) report extremely high fluid flow rates (30–100 cm year^{-1}) and methane fluxes (30–90 $\text{mmol CH}_4 \text{ m}^{-2} \text{day}^{-1}$) in sediments harboring bacterial mats at Hydrate Ridge. Sulfate reduction rates in *Beggiatoa* mat samples from Hydrate Ridge were also extremely high (140 $\text{mmol m}^{-2} \text{day}^{-1}$, Boetius et al., 2000). Rates of AOM were not measured directly but were inferred to be extremely high (Hinrichs and Boetius, 2002).

Rates of SR and AOM in Gulf of Mexico seep samples greatly exceed rates in non-seep habitats in the Gulf of Mexico and elsewhere. Lin and Morse (1991) report SR rates of 2.1 $\text{mmol m}^{-2} \text{day}^{-1}$ along the Texas Shelf and 13 $\text{mmol m}^{-2} \text{day}^{-1}$ along the Mississippi River Delta. Arvidson et al. (in press) showed that SR rates in Gulf of Mexico seep sediments exceeded those available from any other habitats, including intertidal microbial mats (about 150 $\text{mmol m}^{-2} \text{day}^{-1}$, Canfield and Des Marais, 1993) and coastal salt marshes (40 to $>100 \text{ mmol m}^{-2} \text{day}^{-1}$, King et al., 1985; Kostka et al., 2002). Our SR rates are similar to those reported by Arvidson. The AOM rates reported here are about 2–10 times the average rates reported for nearshore, shelf, or margin sediments (range: 0.2 to 2.8 $\text{mmol m}^{-2} \text{day}^{-1}$, Hinrichs and Boetius, 2002). However, the rates determined in tracer studies at other methane seeps are similar to the rates reported here (about 5 $\text{mmol m}^{-2} \text{day}^{-1}$, Bussman et al., 1999; Lein et al., 2000).

In diffusion-dominated gas hydrate provinces, such as the Blake Ridge, AOM and SR appear to be tightly

coupled (Hoehler et al., 2000; Borowski et al., 1996, 1999). In laboratory studies, a 1:1 stoichiometry for AOM and SR was documented in sediments from a hydrate environment where methane was the only carbon source (Nauhaus et al., 2002). Using a 1:1 stoichiometry for SR and AOM at our study sites would have overestimated AOM by about a factor of 10. This overestimation results from the loose coupling between AOM and SR at Gulf of Mexico seep sites, which is caused by the availability of other labile hydrocarbons in addition to methane.

A variety of short- and long-chain alkanes and complex aliphatic and aromatic compounds can be oxidized by sulfate reducing bacteria (Rueter et al., 1994; Heider et al., 1999; Spormann and Widdel, 2000); many such compounds are abundant in Gulf of Mexico seep sediments. For example, in addition to C₁–C₅ alkanes and oil (oil concentrations can be >500 ppm; Kennicutt et al., 1988a,b), a wide variety of other alkanes, alkenes and alkylbenzenes are present in Gulf of Mexico sediments (e.g., hexadecane, naphthalene, phenanthrene, toluene, etc.; Kennicutt et al., 1988a,b). It is likely that most of the SR we measured was coupled to the oxidation of hydrocarbons other than methane, as evidenced by the imbalance between SR and AOM rates. Even for a substrate like toluene, oxidation coupled to sulfate reduction yields more energy (about –205 kJ per mole of substrate oxidized; Heider et al., 1999) than syntrophic AOM (about –25 kJ per mole of substrate oxidized). It is reasonable and probable that the oxidation of other deep reservoir derived hydrocarbons supported a substantial fraction of the SR we measured at active seep sites in the Gulf of Mexico.

Combining the size of CH₄ and SO₄²⁻ pools with the rates of oxidation and reduction, respectively, allowed us to estimate pool turnover times (Table 3). The turnover time for the CH₄ pool was short, being days to weeks, even in inactive control cores. Even low seepage control cores that had low pore water CH₄ concentrations (<5 μM) exhibited efficient consumption of methane as it diffused through the sediment. In active seep samples, surface (0–2 cm) concentrations of CH₄ were also low (<25 μM) but deep (>10 cm) concentrations were high (>1000 μM), illustrating efficient consumption by AOM over depth. Rapid turnover time for the CH₄ pool suggests that AOM rates are CH₄-limited in this system. In

contrast, the turnover time of the SO₄²⁻ pool varied with the SR rate: in cores with high SR rates, the pool turnover time was weeks while in cores with lower rates, the SO₄²⁻ turnover time was weeks to years. This suggests that SR rates may be limited by organic carbon availability (in cores with low rates) or by SO₄²⁻ availability (in cores with high rates).

Methane-limited AOM infers that AOM is controlled strongly by factors that influence pore water CH₄ concentrations, such as the fluid advection rate and gas hydrate stability. All sediment microbial communities were poised to consume CH₄ efficiently and at high fluxes (generating high CH₄ concentrations), AOM could become oxidant limited (see below). Seepage rates will also influence SR rates, such that high fluxes of labile hydrocarbons drive SR rates towards SO₄²⁻ limitation. Likewise, low seepage rates may limit SR and AOM by reducing the availability of carbon substrates. The activity of VSBs, both in terms of H₂S oxidation and by potentially mixing of pore fluids, could impact rates of both AOM and SR by increasing the SO₄²⁻ supply to sulfate reducers. Gas bubbles streaming from sediments are a common feature at Gulf of Mexico cold seeps. So, enhanced substrate transport by fluid advection, by the activity of VSBs, or by bubble-induced pore water mixing (O'Hara et al., 1995) may act in concert to maintain the CH₄ and SO₄²⁻ concentrations required to sustain the rates of turnover we documented.

The co-migration of oil and gas creates a unique biogeochemical regimes at Gulf of Mexico cold seeps. Both TOC and carbonate δ¹³C data and the lack of 1:1 coupling between SR and AOM suggest that the majority of SR at seep sites was fueled by the oxidation of other hydrocarbons and oil; only a small fraction of SR was coupled to AOM (Table 2). The δ¹³C of carbonate was lightest in cores from active hydrate-dominated sites (Table 3). At seep sites, if excess pore water DIC δ¹³C was derived solely from AOM, the δ¹³C-DIC would be expected to be similar to venting CH₄ or hydrate-derived CH₄, which have similar δ¹³C values, with the δ¹³C-DIC eventually approaching that of the CH₄ being oxidized (Aharon, 2000). This would result in the precipitation of ¹³C-depleted carbonates. Though the δ¹³C-carbonate is lighter than the expected carbonates derived from precipitation of seawater DIC (0‰ to +2‰, Kump

and Arthur, 1999), the $\delta^{13}\text{C}$ -carbonate is not driven solely by methane (-45‰ , Sassen et al., 1999), again suggesting that oxidation of other hydrocarbon or oil (-28‰) provides the bulk of pore water DIC that precipitates as authigenic carbonates.

5. Conclusions and summary

Despite the abundance of methane at cold seeps in the Gulf of Mexico, coupling between AOM and SR is weak and AOM accounts for only a small fraction of SR activity observed in the sediments. In this system, CH_4 is just one of a diverse suite of seep-derived organic substrates that could fuel sulfate reduction (Brooks et al., 1984; Aharon, 2000). A variety of long-chain alkanes, complex aliphatic and aromatic compounds, and oils can be consumed by sulfate reducing bacteria and in this system. The lack of strong (1:1) coupling between AOM and SR means that SR in Gulf of Mexico seep sediments must be driven by the oxidation of other organic compounds more so than by AOM.

The magnitude of spatial and temporal variation in fluid flow at Gulf of Mexico seeps is presently unknown. Fluid flow data from Hydrate Ridge show that temporal and spatial variations in seepage occur (Torres et al., 2002; Tyron et al., 2002) and similarly variable flow rates might be expected at Gulf of Mexico cold seeps. The inherent variability in seepage rate, and hence in substrate supply, may select for a metabolically plastic microbial community that is adept at consuming a variety of organic substrates when CH_4 is limiting but one that is also poised to take advantage of periods when CH_4 is available. Furthermore, the presence of other, more energetically favorable substrates could generate competition for available sulfate between microbes involved in AOM and microbes oxidizing other hydrocarbons and oil. Such competition could serve to structure the microbial community at mixed substrate (gas- and petroleum-rich) cold seeps. The capacity for AOM in such sediments and the impact of other reduced carbon substrates on AOM rates should be examined carefully in laboratory experiments to better elucidate the biogeochemical and microbiological controls on AOM in situ. Despite the presence of alternate reduced carbon substrates, Gulf of Mexico seep

sediments harbor anaerobic methane-consuming microorganisms that act as an efficient biofilter preventing methane emission to the hydrosphere, except at a few sites where hydrate dissociation and fluid flow create so much gas pressure that free gas emanates from the sediments in the form of gas bubbles.

Acknowledgements

We thank members of the LExEn 2001 scientific party; in particular, we acknowledge I. MacDonald, S. de Beukelaer, and M. Vardaro for assistance with preparing and handling sediment cores, S. de Beukelaer for providing the map presented in Fig. 1, C. Payne for assistance with stable isotope analyses, and C. Meile and two anonymous reviewers for providing critical comments that improved this manuscript significantly. We thank the crew of the *R/V Seward Johnson*, and the pilots and crew of the deep submergence vehicle *Johnson Sea Link* for assistance with sample collection. The US Department of Energy and the National Undersea Research Program provided funding for submersible operations. The National Science Foundation (OCE-0085549), the American Chemical Society (PRF-36834-AC2), the German Federal Ministry for Education and Research (project MUMM, BMBF-03G0554A), the Max Planck Society, a post-doctoral fellowship (to HNS) from the German Science Foundation (DFG), and a sabbatical fellowship (to SBJ) from the Hanse Institute for Advanced Study, Delmenhorst, Germany provided funding for this work and for the preparation of this manuscript. This is publication number 18 of the GEOTECHNOLOGIEN program of BMBF and DFG. [LW]

References

- Aharon, P., 1994. Geology and biology of modern and ancient submarine hydrocarbon seeps and vents: an introduction. *Geo Mar. Lett.* 14, 69–73.
- Aharon, P., 2000. Microbial processes and products fueled by hydrocarbons at submarine seeps. In: Riding, R.E., Awramik, S.M. (Eds.), *Microbial Sediments*. Springer-Verlag, Berlin, pp. 270–281.
- Aharon, P., Fu, B., 2000. Microbial sulfate reduction rates and

- sulfur and oxygen isotope fractionations at oil and gas seeps in deepwater Gulf of Mexico. *Geochim. Cosmochim. Acta* 64, 233–246.
- Aharon, P., Roberts, H.H., Snelling, R., 1992. Submarine venting of brines in the deep Gulf of Mexico: observations and geochemistry. *Geology* 20, 483–486.
- Ahmad, A., Barry, J.P., Nelson, D.C., 1999. Phylogenetic affinity of a wide, vacuolate, nitrate-accumulating *Beggiatoa* sp., from Monterey Canyon California, with *Thioploca* spp. *Appl. Environ. Microbiol.* 65, 270–277.
- Alperin, M.J., Reeburgh, W.S., Whiticar, M.J., 1988. Carbon and hydrogen isotope fractionation resulting from anaerobic methane oxidation. *Glob. Biogeochem. Cyc.* 2, 279–288.
- Anderson, R.K., Scalan, R.S., Parker, P.L., 1983. Seep oil and gas in Gulf of Mexico slope sediments. *Science* 222, 619–622.
- Arvidson, R., Morse, J.W., Joyce, S.B., 2004. The sedimentary biogeochemistry of chemosynthetic cold seep communities, Gulf of Mexico, USA, *Marine Chemistry*, in press.
- Ashi, J., Tokuyama, H., Taira, A., 2002. Distribution of methane hydrate BSRs and its implication for the prism growth in the Nankai Trough. *Mar. Geol.* 187, 177–191.
- Barry, J.P., Greene, H.G., Orange, D.L., Baxter, C.H., Robison, B.H., Kochevar, R.E., Nybakken, J.W., Reed, D.L., McHugh, C.M., 1996. Biologic and geologic characteristics of cold seeps in Monterey Bay California. *Deep-Sea Res.* 43, 1739–1762.
- Behrens, E.W., 1980. On sedimentation rates and porosity. *Mar. Geol.* 35, 12–16.
- Behrens, E.W., 1988. Geology of a continental slope oil seep, northern Gulf of Mexico. *AAPG Bull.* 72, 105–114.
- Boetius, A., Ravensschlag, K., Shubert, C.J., Rickert, D., Widdel, F., Gieseke, A., Amann, R., Jørgensen, B.B., Witte, U., Pfannkuche, O., 2000. Microscopic identification of a microbial consortium apparently mediating anaerobic methane oxidation above marine gas hydrates. *Nature* 407, 623–626.
- Borowski, W.S., Paull, C.K., Ussler III, W., 1996. Marine pore-water sulfate profiles indicate in situ methane flux from underlying gas hydrate. *Geology* 24, 655–658.
- Borowski, W.S., Paull, C.K., Ussler III, W., 1999. Global and local variations of interstitial sulfate gradients in deep-water, continental margin sediments; sensitivity to underlying methane and gas hydrates. *Mar. Geol.* 159, 31–154.
- Brooks, J.M., Kennicutt III, M.C., Fay, R.R., McDonald, T.J., Sassen, R., 1984. Thermogenic gas hydrates in the Gulf of Mexico. *Science* 223, 696–698.
- Brooks, J.M., Kennicutt II, M.C., Fisher, C.R., Macko, S.A., Cole, K., Childress, J.J., Bidigare, R.R., Vetter, R.D., 1987. Deep-sea hydrocarbon seep communities: evidence for energy and nutritional carbon sources. *Science* 238, 1138–1142.
- Brown, K.M., Bangs, N.L., Froelich, P.N., Kvenvolden, K.A., 1996. The nature and origin of the bottom simulating reflector and associated gas hydrate in the Chile triple junction region. *Earth Planet. Sci. Lett.* 139, 471–483.
- Bussman, I., Dando, P.R., Niven, S.J., Suess, E., 1999. Groundwater seepage in the marine environment: role for mass flux and bacterial activity. *Mar. Ecol., Prog. Ser.* 178, 169–177.
- Canfield, D.E., Des Marais, D.J., 1993. Biogeochemical cycles of carbon, sulfur, and free oxygen in a microbial mat. *Geochim. Cosmochim. Acta* 57, 3971–3984.
- Canfield, D.E., Raiswell, R., Westrich, J.T., Reaves, C.M., Berner, R.A., 1986. The use of chromium reduction in the analysis of reduced inorganic sulfur in sediments and shales. *Chem. Geol.* 54, 149–155.
- Carney, R.S., 1994. Consideration of the oasis analogy for chemosynthetic communities at Gulf of Mexico hydrocarbon vents. *Geo Mar. Lett.* 14, 149–159.
- Childress, J.J., Fisher, C.R., Brooks, J.M., Kennicutt II, M.C., Bidigare, R.R., Anderson, A., 1986. A methanotrophic marine molluscan (*Bivalvia*, *Mytilidae*) symbiosis: mussels fueled by gas. *Science* 233, 1306–1308.
- Claypool, G.E., Kaplan, I.R., 1974. The origin and distribution of methane in marine sediments. In: Kaplan, I.R. (Ed.), *Natural Gases in Marine Sediments*. Plenum, New York, pp. 99–139.
- Cline, J.D., 1969. Spectrophotometric determination of hydrogen sulfide in natural waters. *Limnol. Oceanogr.* 14, 454–458.
- Collett, T.S., Kuuskraa, V.A., 1998. Hydrates contain vast store of world gas resources. *Oil Gas J.* 96 (19), 90–95.
- Davis, R.W., Ortega-Ortiz, J.G., Ribic, C.A., Evans, W.E., Biggs, D.C., Ressler, P.H., Cady, R.B., Leben, R.R., Mullin, K.D., Wursig, B., 2002. Cetacean habitat in the northern oceanic Gulf of Mexico. *Deep Sea Res.* 49, 121–142.
- de Angelis, M.A., Reysenback, A.-L., Baross, J.A., 1991. Surfaces of hydrothermal vent invertebrates: sites of elevated microbial methane oxidation activity. *Limnol. Oceanogr.* 36, 570–577.
- Devol, A.H., Anderson, J.J., Kuivila, K.M., Murray, J.W., 1984. A model for coupled sulfate reduction and methane oxidation in the sediments of Saanich Inlet. *Geochim. Cosmochim. Acta* 48, 993–1004.
- Dickens, G.R., O'Neil, J.R., Rea, D.K., Owen, R.M., 1995. Dissociation of oceanic methane hydrate as a cause of the carbon isotope excursion at the end of the Paleocene. *Paleoceanography* 10 (6), 965–971.
- Dickens, G.R., Paull, C.K., Wallace, P., ODP Leg 164 Scientific Party, P., 1997. Direct measurement of in situ methane quantities in a large gas-hydrate reservoir. *Nature* 385, 426–428.
- Ferrell, R.E., Aharon, P., 1994. Mineral assemblages occurring around hydrocarbon vents in the northern Gulf of Mexico. *Geo Mar. Lett.* 14, 74–80.
- Fisher, C.R., 1990. Chemoautotrophic and methanotrophic symbioses in marine invertebrates. *Crit. Rev. Aqu. Sci.* 2, 399–436.
- Fossing, H., Jørgensen, B.B., 1989. Measurement of bacterial sulfate reduction in sediments: evaluation of a single-step chromium reduction method. *Biogeochem* 8, 205–222.
- Fossing, H.A., Gallardo, V.A., Jørgensen, B.B., Hüttel, M., Nielsen, L.P., Schulz, H.N., Canfield, D.E., Forster, S., Glud, R.N., Gundersen, J.K., Küver, J., Ramsing, N.B., Teske, A., Thamdrup, O., Ulloa, O., 1995. Concentration and transport of nitrate by the mat-forming sulphur bacterium *Thioploca*. *Nature* 374, 713–715.
- Goñi, M.A., Ruttenger, K.C., Eglinton, T.I., 1998. A reassessment of the sources and importance of land-derived organic matter in surface sediments from the Gulf of Mexico. *Geochim. Cosmochim. Acta* 62, 3055–3075.
- Gundersen, J.K., Jørgensen, B.B., Larsen, E., Jannasch, H.W.,

1992. Mats of giant sulphur bacteria on deep sea sediments due to fluctuating hydrothermal flow. *Nature* 360, 454–456.
- Hackworth, M., Aharon, P., 2002. Determination of sedimentation rates in Gulf of Mexico gas hydrate-bearing sediments using radiocarbon and stable carbon isotopes. *Nat. Geol. Soc. Amer. Meeting*, Denver, Colorado. Published abstract.
- Heider, J., Spormann, A.M., Beller, H.R., Widdel, F., 1999. Anaerobic bacterial metabolism of hydrocarbons. *FEMS Microbiol. Rev.* 22, 459–473.
- Hesselbo, S.P., Gröcke, D.R., Jenkyns, H.C., Bjerrum, C.J., Farnmond, P., Morgans Bell, H.S., Green, O.R., 2000. Massive dissociation of gas hydrate during a Jurassic oceanic anoxic event. *Nature* 406, 392–395.
- Hinrichs, K.-U., Boetius, A., 2002. The anaerobic oxidation of methane: New insights in microbial ecology and biogeochemistry. In: Wefer, G., Billett, D., Hebbeln, D., Jørgensen, B.B., Schlüter, M., van Weering, T.C.E. (Eds.), *Ocean Margin Systems*. Springer-Verlag, Berlin, pp. 457–477.
- Hinrichs, K.U., Hayes, J.M., Sylva, S.P., Brewster, P.G., DeLong, E.F., 1999. Methane-consuming archaeobacteria in marine sediments. *Nature* 398, 802–805.
- Hoehler, T.M., Alperin, M.J., 1996. Anaerobic methane oxidation by a methanogen-sulfate reducer consortium: Geochemical evidence and biochemical considerations. In: Lindstrom, M.E., Tabita, F.R. (Eds.), *Microbial Growth on C₁ Compounds*. Kluwer Academic Publishing, The Netherlands, pp. 326–333.
- Hoehler, T.M., Alperin, M.J., Albert, D.B., Martens, C.S., 1994. Field and laboratory studies of methane oxidation in an anoxic marine sediment; evidence for a methanogen-sulfate reducer consortium. *Glob. Biogeochem. Cycles* 8, 451–463.
- Hoehler, T.M., Borowski, W.S., Alperin, M.J., Rodriguez, N.M., Paull, C.K., 2000. Model, stable isotope, and radiotracer characterization of anaerobic methane oxidation in gas hydrate-bearing sediments of the Blake Ridge. In: Paull, C.K., Matsumoto, R., Wallace, P.J., Dillon, W.P. (Eds.), *Proceedings of the Ocean Drilling Program, Scientific Results*, vol. 164. Ocean Drilling Program, College Station, TX, pp. 79–85.
- Hoehler, T.M., Alperin, M.J., Albert, D.B., Martens, C.S., 2001. Apparent minimum free energy requirements for methanogenic Archaea and sulfate-reducing bacteria in an anoxic marine sediment. *FEMS Microbiol. Ecol.* 38, 33–41.
- Iversen, N., Jørgensen, B.B., 1985. Anaerobic methane oxidation rates at the sulfate-methane transition in marine sediments from the Kattegat and Skagerrack (Denmark). *Limnol. Oceanogr.* 30, 944–955.
- Jannasch, H.W., Nelson, D.C., Wirsén, C.O., 1989. Massive natural occurrence of unusually large bacteria (*Beggiatoa* sp.) at a hydrothermal deep-sea vent site. *Nature* 342, 834–836.
- Jeroschewski, P., Steuckart, C., Köhl, M., 1996. An amperometric microsensor for the determination of H₂S in aquatic environments. *Anal. Chem.* 68, 4351–4357.
- Jørgensen, B.B., 1978. A comparison of methods for the quantification of bacterial sulfate reduction in coastal marine sediments. *Geomicrobiology* 1, 11–27.
- Jørgensen, B.B., Gallardo, V.A., 1999. *Thioploca* spp: filamentous sulfur bacteria with nitrate vacuoles. *FEMS Microbiol. Ecol.* 28, 301–313.
- Jørgensen, B.B., Revsbech, N.P., 1983. Colorless sulfur bacteria, *Beggiatoa* spp. and *Thiovulum* spp., in O₂ and H₂S microgradients. *Appl. Environ. Microbiol.* 45, 1261–1270.
- Joye, S.B., Connell, T.L., Miller, L.G., Oremland, R.S., 1999. Oxidation of ammonia and methane in an alkaline, saline lake. *Limnol. Oceanogr.* 44, 178–188.
- Judd, A.G., Sim, R., Kingston, P., McNally, J., 2002. Gas seepage on an intertidal site: Torry Bay Firth of Forth, Scotland. *Cont. Shelf Res.* 22, 2317–2331.
- Kahn, L.M., Silver, E.A., Orange, D.L., Kochevar, R., McAdoo, B.G., 1996. Surficial evidence of fluid expulsion from the Costa Rica accretionary prism. *Geophys. Res. Lett.* 23, 887–890.
- Katz, M.E., Pak, D.K., Dickens, G.R., Miller, K.G., 1999. The source and fate of massive carbon input during the latest Paleocene thermal maximum. *Science* 286, 1531–1533.
- Kennett, J.P., Cannariato, K.G., Hendy, I.L., Behl, R.J., 2000. Carbon isotopic evidence for methane hydrate instability during quaternary interstadials. *Science* 288, 128–133.
- Kennicutt, M.C., Brooks, J.M., Bidigare, R.R., Fay, R.R., Wade, T.L., MacDonald, T.J., 1985. Vent-type taxa in a hydrocarbon seep region on the Louisiana slope. *Nature* 317, 351–353.
- Kennicutt, M.C., Brooks, J.M., Denoux, G.J., 1988a. Leakage of deep, reservoired petroleum to the near surface on the Gulf of Mexico continental slope. *Mar. Chem.* 24, 39–59.
- Kennicutt, M.C., Brooks, J.M., Bidigare, R.R., Denoux, G.J., 1988b. Gulf of Mexico hydrocarbon seep communities: I. Regional distribution of hydrocarbon seepage and associated fauna. *Deep-Sea Res.* 35A, 1639–1651.
- King, G.M., Howes, B.L., Dacey, J.W.H., 1985. Short-term end products of sulfate reduction in a salt marsh; formation of acid volatile sulfides, elemental sulfur, and pyrite. *Geochim. Cosmochim. Acta* 49, 1561–1566.
- Kostka, J.E., Roychoudhury, A., Van Cappellen, P., 2002. Rates and controls of anaerobic microbial respiration across spatial and temporal gradients in saltmarsh sediments. *Biogeochemistry* 60, 49–76.
- Kump, L.R., Arthur, M.A., 1999. Interpreting carbon-isotope excursions: carbonates and organic matter. *Chem. Geol.* 161, 181–198.
- Kvenvolden, K.A., 1988. Methane hydrates and global change. *Glob. Biogeochem. Cycles* 2 (3), 221–229.
- Kvenvolden, K.A., 1993. Gas hydrates—geological perspective and global change. *Rev. Geophys.* 31, 173–187.
- Larkin, J., Aharon, P., Henk, M.C., 1994. *Beggiatoa* in microbial mats at hydrocarbon vents in the Gulf of Mexico and Warm Mineral Springs, Florida. *Geo Mar. Lett.* 14, 97–103.
- Lein, A., Pimenov, N.V., Savvichev, A.S., Pavlova, G.A., Vogt, P.R., Bogdanov, Y.A., Sagalevich, A.M., Ivanov, M.V., 2000. Methane as a source of organic matter and carbon dioxide of carbonates at a cold seep in the Norway Sea. *Geochem. Int.* 38, 232–245.
- Lin, S., Morse, J.W., 1991. Sulfate reduction and iron sulfide mineral formation in Gulf of Mexico anoxic sediments. *Am. J. Sci.* 291, 55–89.
- MacAvoy, S.A., Macko, S.A., Joye, S.B., 2002. Fatty acid carbon isotope signatures in chemosynthetic mussels and tube worms from Gulf of Mexico hydrocarbon seep communities. *Chem. Geol.* 185, 1–8.

- MacDonald, I.R., Boland, G.S., Baker, J.S., Brooks, J.M., Kennicutt II, M.C., Bidigare, R.R., 1989. Gulf of Mexico chemosynthetic communities II: spatial distribution of seep organisms and hydrocarbons at Bush Hill. *Mar. Biol.* 101, 235–247.
- MacDonald, I.R., Guinasso, N.L., Reilly, J.F., Brooks, J.M., Callender, W.R., Gabrielle, S.G., 1990. Gulf of Mexico Hydrocarbon Seep Communities VI: species composition and habitat characteristics. *Geo Mar. Lett.* 10, 244–252.
- MacDonald, I.R., Reilly Jr., J.F., Best, S.E., Venkataramaiah, R., Sassen, R., Amos, J., Guinasso Jr., N.L., 1996. A remote-sensing inventory of active oil seeps and chemosynthetic communities in the northern Gulf of Mexico. In: Schumacher, D., Abrams, M.A. (Eds.), *Hydrocarbon Migration and its Near-Surface Expression*. AAPG Memoir 66, 22–37.
- McHatton, S.C., Barry, J.P., Jannasch, H.W., Nelson, D.C., 1996. High nitrate concentrations in vacuolate, autotrophic marine *Beggiatoa* spp. *Appl. Environ. Microbiol.* 62, 954–958.
- Michaelis, W., Seifert, R., Nauhaus, K., Treude, T., Thiel, V., Blumenberg, M., Knittel, K., Gieseke, A., Peterknecht, K., Pape, T., Boetius, A., Amann, R., Jørgensen, B.B., Widdel, F., Peckmann, J., Pimenkov, N., Gulin, M.B., 2002. Microbial reefs in the black sea fueled by anaerobic methane oxidation. *Science* 297, 1013–1015.
- Nauhaus, K., Boetius, A., Krüger, M., Widdel, F., 2002. *In vitro* demonstration of anaerobic oxidation of methane coupled to sulfate reduction from a marine gas hydrate area. *Environ. Microbiol.* 4, 296–305.
- Nelson, D.C., Jannasch, H.W., 1983. Chemoautotrophic growth of a marine *Beggiatoa* in sulfide-gradient cultures. *Arch. Microbiol.* 136, 262–269.
- Nelson, D.C., Revsbech, N.P., Jørgensen, B.B., 1986. Microoxic-anoxic niche of *Beggiatoa* spp.: microelectrode survey of marine and freshwater strains. *Appl. Environ. Microbiol.* 52, 161–168.
- Norris, R.D., Röhl, U., 1999. Carbon cycling and chronology of climate warming during the Paleocene/Eocene transition. *Nature* 401, 775–778.
- O'Hara, S.C.M., Dando, P.R., Schuster, U., Bennis, A., Boyle, J.D., Chiu, F.T.W., Hatherell, T.V.J., Niven, S.J., Taylor, L.J., 1995. Gas seep induced interstitial water circulation: observations and environmental implications. *Cont. Shelf Res.* 15, 931–948.
- Orcutt, B.N., Boetius, A., Lugo, S.K., MacDonald, I.R., Samarkin, V., Joye, S.B., 2004. Life at the edge of methane ice: methane and sulfur cycling in Gulf of Mexico gas hydrates. *Chem. Geol.* this issue.
- Orphan, V.J., Hinrichs, K.-U., Ussler III, W., Paull, C.K., Taylor, L.T., Sylva, S.P., Hayes, J.M., DeLong, E.F. 2001a. Comparative analysis of methane-oxidizing archaea and sulfate-reducing bacteria in anoxic marine sediments. *Appl. Environ. Microbiol.* 67, 1922–1934.
- Orphan, V.J., House, C.H., Hinrichs, K.-U., McKeegan, K.D., DeLong, E.F., 2001b. Methane-consuming archaea revealed by directly coupled isotopic and phylogenetic analysis. *Science* 293, 484–487.
- Otte, S., Kuenen, J.G., Nielsen, L.P., Paerl, H.W., Zopf, J., Schulz, H.N., Teske, A., Strotmann, B., Gallardo, V.A., Jørgensen, B.B., 1999. Nitrogen, carbon, and sulfur metabolism in natural *Thioploca* samples. *Appl. Environ. Microbiol.* 65, 3148–3157.
- Paull, C.P., Ussler, W., Dillon, W., 1991. Is the extent of glaciation limited by methane gas-hydrates? *Geophys. Res. Lett.* 18, 432–434.
- Reeburgh, W.S., 1967. An improved interstitial water samples. *Limnol. Oceanogr.* 12, 163–165.
- Reeburgh, W.S., 1976. Methane consumption in cariac trench waters and sediments. *Earth Planet. Sci. Lett.* 28, 227–244.
- Roberts, H.H., Carney, R.S., 1997. Evidence of episodic fluid, gas, and sediment venting on the northern Gulf of Mexico continental slope. *Econ. Geol.* 92, 863–879.
- Roberts, H.H., McBride, R.A., Coleman, J., 1999. Outer shelf and slope geology of the Gulf of Mexico: an overview. In: Kumpf, H., Steidinger, K., Sherman, K. (Eds.), *The Gulf of Mexico Large Marine Ecosystems: Assessment, Sustainability, and Management*. Blackwell Science Ltd, pp. 93–112.
- Rueter, P., Rabus, R., Wilkes, H., Aeckersberg, F., Rainey, F.A., Jannasch, H.W., Widdel, F., 1994. Anaerobic oxidation of hydrocarbons in crude oil by denitrifying bacteria. *Nature* 372, 455–458.
- Sassen, R., Roberts, H., Aharon, R., Larkin, J., Chinn, E., Carney, R., 1993. Chemosynthetic bacterial mats at cold hydrocarbon seeps Gulf of Mexico continental slope. *Org. Geochem.* 20, 77–89.
- Sassen, R., MacDonald, I.R., Requejo, A.G., Guinasso, N.L., Kennicutt, M.C., Sweet, S.T., Brooks, J.M., 1994. Organic geochemistry of sediments from chemosynthetic communities Gulf of Mexico slope. *Geo Mar. Lett.* 14, 110–119.
- Sassen, R., MacDonald, I.R., Guinasso, N.J., Joye, S.B., Requejo, A.G., Sweet, S.T., Alcalá-Herrera, J., DeFreitas, D.A., Schink, D.R., 1998. Bacterial methane oxidation in sea-floor gas hydrate: Significance to life in extreme environments. *Geology* 26, 851–854.
- Sassen, R., Joye, S., Sweet, S.T., DeFreitas, D.A., Milkov, A.V., MacDonald, I.R., 1999. Thermogenic gas hydrates and hydrocarbon gases in complex chemosynthetic communities Gulf of Mexico continental slope. *Org. Geochem.* 30, 485–497.
- Soloranzo, L., 1969. Determination of ammonia in natural waters by the phenol hypochlorite method. *Limnol. Oceanogr.* 14, 799–801.
- Spormann, A.M., Widdel, F., 2000. Metabolism of alkylbenzenes, alkanes, and other hydrocarbons in anaerobic bacteria. *Biodegradation* 11, 85–105.
- Sweerts, J.-P.R.A., De Beer, D., Nielsen, N.P., Verdouw, H., Heuvel, J.C.V., Cohen, Y., Cappenberg, T.E., 1990. Denitrification by sulfur oxidizing *Beggiatoa* spp. mats on freshwater sediments. *Nature* 344, 762–763.
- Suess, E., Torres, M.E., Bohrmann, G., Collier, R.W., Greinert, J., Linke, P., Rehder, G., Trehu, A., Wallmann, K., Winckler, G., Zuleger, E., 1999. Gas hydrate destabilization: enhanced dewatering, benthic material turnover, and large methane plumes at the Cascadia convergent margin. *Earth Planet. Sci. Lett.* 170, 1–15.
- Torres, M.E., McManus, J., Hammond, D.E., de Angelis, M.A., Heeschen, K.U., Colbert, S.L., Tyron, M.D., Brown, K.M., Suess, E., 2002. Fluid and chemical fluxes in and out of

- sediments hosting methane hydrate deposits on hydrate ridge, OR I: hydrological provinces. *Earth Planet. Sci. Lett.* 201, 525–540.
- Tsunogai, U., Yoshida, N., Gamo, T., 2002. Carbon isotopic evidence of methane oxidation through sulfate reduction in sediment beneath cold seep vents on the seafloor at Nankai Trough. *Mar. Geol.* 187, 145–160.
- Tyron, M.D., Brown, K.M., Torres, M.E., 2002. Fluid and chemical flux in and out of sediments hosting methane hydrate deposits on Hydrate Ridge, OR II: Hydrological processes. *Earth Planet. Sci. Lett.* 201, 541–557.